

## Single Molecule Experiments Visualizing Adsorbed Polyelectrolyte Molecules in the Full Range of Mono- and Divalent Counterion Concentrations

Yuri Roiter, Oleksandr Trotsenko, Viktor Tokarev,<sup>†</sup> and Sergiy Minko\*

Department of Chemistry and Biomolecular Science, Clarkson University, 8 Clarkson Avenue, Potsdam, New York 13699

Received July 16, 2010; E-mail: sminko@clarkson.edu

**Abstract:** This work provides direct experimental verification (on the level of single molecules) for the behavior of hydrophobic polyelectrolyte chains adsorbed at a solid–liquid interface in the full range of possible salt concentrations: (a) in a dilute salt solution, PE chains possess an extended coil conformation visualized as adsorbed 2D-equilibrated coils; (b) in a moderate salt concentration range, the polymer coil shrinks and approaches the dimensions of a polymer coil under  $\theta$ -conditions and the chains are visualized as adsorbed 3D-projected coils; (c) at high salt concentrations, the polymer coils reexpand and the molecules are visualized as 2D-equilibrated extended coils; however, (d) reexpansion is limited in the presence of multivalent counterions, presumably due to the bridging of the polymer coils by the counterions.

This work presents the first direct experimental visualization of adsorbed polyelectrolyte (PE) single molecule conformations in the presence of monovalent and multivalent salts in a broad range of salt concentrations from very diluted to highly concentrated (close to the solubility limit) solutions using *in situ* atomic force microscopy (AFM).

PEs are synthetic and natural polymers carrying electrical charges of ionized functional groups in liquids of high dielectric constants. They are very important for living organisms, water purification, and many industrial technologies, such as cosmetics, medicine, and agriculture. Understanding the properties of PE molecules in different environments is critical for many applications. Hydrophobic PEs (HPEs) consist of a hydrophobic backbone with ionizable side functional groups. Conformation of HPE chains in aqueous solutions depends on the balance of repulsive Coulomb and attractive hydrophobic intrachain interactions.<sup>1–3</sup> If an HPE is poorly charged, the hydrophobic interactions result in a compact globule conformation; however, a highly charged HPE possesses an extended coil conformation because of the electrostatic repulsion. In salt solutions, electrostatic interactions are screened and a fraction of counterions are condensed on polymer chains. At a range of moderate ionic strengths (IS = 0.05–0.5 M) hydrophobic PE chains shrink and possess the dimensions of a coil under  $\theta$ -conditions.<sup>4</sup> Simulation and experimental studies have shown that the compaction of PE chains is driven by multivalent counterions more efficiently than by monovalent counterions (MC) at the same IS.<sup>5,6</sup> It is likely that a combination of weakened electrostatic repulsion between charged functional groups and electrostatic attractions introduced by condensed counterions (ion bridging) is responsible for the collapse of HPE chains at moderate IS.

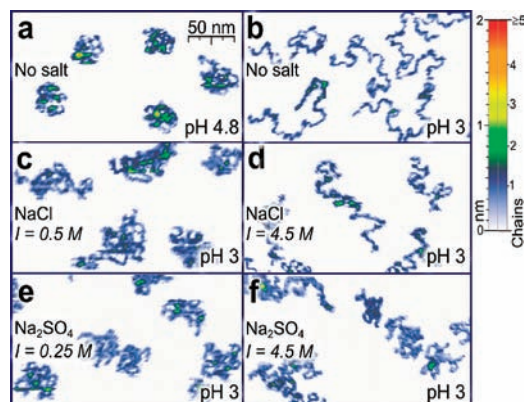


**Figure 1.** AFM images of P2VP molecules under salt-free conditions at pH 4.8 (a) and 3.0 (b) and at the moderate to high values of IS (shown in images) in NaCl (c, d) and Na<sub>2</sub>SO<sub>4</sub> (e, f) solutions; 50 nm scale bar shown in (a) is valid for all images. Z-scale is shown in colors; the Z-scale bar (on the right) shows a number of superposed segments with an assumption of a 0.4 nm height increment (diameter of the backbone).

Simulations and theoretical analysis<sup>2,7–11</sup> demonstrated that a further increase of the ionic strength leads to the phenomena known as chain reexpansion or redissolution, usually explained by the increasing quantity of counterions condensed on the PE chain. For example, Nguyen et al.<sup>12</sup> presented a theory describing changes of net DNA charge and of the charge sign with increasing concentration of multivalent counterions, leading to DNA condensation, which is followed by its redissolution and inversion of the direction of electrophoretic mobility. Simulations predicted a higher efficiency of multivalent counterions in the reexpansion transition.<sup>13,14</sup> Only a few experimental works have systematically studied the reexpansion phenomenon due to the technical limitations of many experimental methods in conditions of very diluted polymer and highly concentrated saline solutions (DNA redissolution<sup>15</sup> and reexpansion of polystyrene sulfonate using fluorescence correlation spectroscopy<sup>16</sup>).

Preferential condensation of polyvalent counterions on the P2VP backbone has previously been visualized with AFM<sup>17,18</sup> using bulky counterions; however, the effect of counterion condensation on chain conformation was not investigated in these earlier works.

We report here the AFM visualization of two salt-induced conformational transitions of PE chains: (1) collapse and formation of PE globules and (2) reexpansion of the globules at high salt concentrations. Conformations of poly(2-vinylpyridine) (P2VP) HPE chains were studied on atomically flat mica in aqueous solutions of NaCl and Na<sub>2</sub>SO<sub>4</sub> at pH 3 (Figure 1). P2VP ( $M_n = 152\,000$  g/mol,  $M_w/M_n = 1.05$ ) concentration was adjusted in the range of  $10^{-3}$ – $10^{-4}$  g/L (monomer unit concentration [2VP] was  $9.51 \times 10^{-6}$  to  $9.51 \times 10^{-7}$  mol/L). The pH was adjusted using HCl and H<sub>2</sub>SO<sub>4</sub>. The experiment was conducted in the following

<sup>†</sup> Permanent address: Lviv Polytechnic National University, 3/4 St. Yura Sq., Lviv, Ukraine.

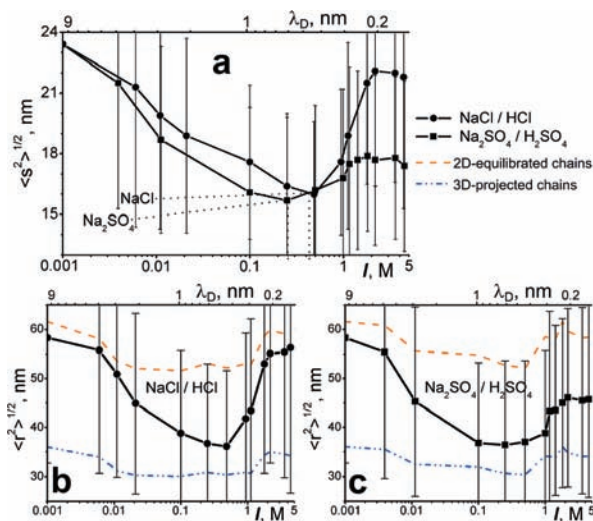


**Figure 2.** Dimensions of adsorbed P2VP molecules vs IS and Debye length ( $\lambda_D$ ) in salt solutions:  $\langle s^2 \rangle^{1/2}$  (a);  $\langle r^2 \rangle^{1/2}$  in NaCl (b) and  $\text{Na}_2\text{SO}_4$  (c) solutions at pH 3.0. The experimental data were averaged for about 200 individual molecules. Red dash and blue dash-dot lines (b–c) display estimated  $\langle r^2 \rangle^{1/2}$  values for 2D-equilibrated and 3D-projected chains, respectively. All lines are given to guide the reader. Standard deviation bars reflect the characteristic distributions of molecules by size (see Supporting Information).

manner. A freshly cleaved disk of mica was mounted in a liquid cell of a MultiMode AFM. The cell was filled with P2VP aqueous solution at the given pH value and salt concentration. The samples were scanned in tapping mode after an incubation period at an amplitude set point in the range from 0.6 to 2.2 V and a tapping force of about 98% of the set point. The statistical analysis of chain conformations was conducted using the previously reported procedure and software (see Supporting Information for details).<sup>19</sup> In the experiments, we examined the conformations of adsorbed P2VP on the mica surface, which reflect the balance of intrachain interactions, and interactions of P2VP chains with water, dissolved salts, and mica. Although the interactions with the mica surface can change the polymer chain conformations, the qualitative features of the coil-to-globule transitions in solution and at the solid–liquid interface are in accord for the P2VP–mica–water system.<sup>17–21</sup>

In unsalted solutions, uncharged P2VP (at pH > 4) molecules possess a compact globule conformation due to hydrophobic interactions (Figure 1a). With a decrease of pH, an increased fraction of protonated and ionized monomeric units forces an expansion of the coils due to strong electrostatic repulsion (Figure 1b)<sup>19</sup> and the addition of salts leads to coil shrinkage (Figure 1c). This transition was shown to pass through a series of intermediate states (in a narrow range of pH or salt concentrations) when the globule is broken into charged hydrophobic beads termed “necklace-like globules.” Necklace-like structures are not stable, so they can only be visualized in special experiments.<sup>20</sup>

Coil-to-globule transition was recorded for both monovalent and divalent salts (Figure 1c, e). Divalent counterions (DC) showed a stronger collapse of the chains in accordance with the theory and results of simulations. This fact is well described by the dependence of the root-mean-square (rms) radius of gyration ( $\langle s^2 \rangle^{1/2}$ ) and rms end-to-end distance ( $\langle r^2 \rangle^{1/2}$ ) values vs the ionic strength from 0.001 M to moderate salt concentrations (Figure 2a–c). The minimal  $\langle s^2 \rangle^{1/2}$  values for P2VP coils were found at 0.43 and 0.25 M ionic strength in NaCl and  $\text{Na}_2\text{SO}_4$  solutions, respectively. Divalent counterions formed more compact globules.

Further addition of salts induced reexpansion of the globules (Figure 1d, f). In contrast to the collapse of coils, the reexpansion

fraction of the plot of coil dimension vs IS is steeper for NaCl solutions than for  $\text{Na}_2\text{SO}_4$  solutions (Figure 2a). This occurrence resulted in a crossing of the plots for MC and DC at 0.43 M IS, when the P2VP coils in both systems are of the same size ( $\langle s^2 \rangle^{1/2} = 16 \pm 3.5$  nm) and correspond to the coil under  $\theta$ -conditions, as reported previously.<sup>21</sup> At higher ionic strengths, NaCl salted globules recover the extended conformation, whereas, for  $\text{Na}_2\text{SO}_4$  solutions, the recovery is only incremental.

This interesting behavior of P2VP chains was examined using statistical analysis of 2D-equilibrated vs 3D-projected chains. The adsorbed polymer chain may occupy either the conformation of the 2D-equilibrated coil, when the interaction with the substrate is sufficiently strong to force the formation of the 2D-coil, or the 3D-projected coil (whose conformation reflects the projection on the solid substrate of the 3D-coil in the solution). In the latter case, the 2D-equilibration is limited by strong intrachain forces. The red and blue dash-dot curves in Figure 2b and c reflect the expected  $\langle r^2 \rangle^{1/2}$  values for polymer chains of the same degree of polymerization in 2D-equilibrated and 3D-projected states, respectively (see Supporting Information). These values were estimated from the experimental values of contour length and persistent length of the examined chains.<sup>22</sup> The data show that P2VP chains occupied the 2D-equilibrated conformation at low (<0.01 M) and at very high (>1M) IS (for MC). In the intermediate range of salt concentrations (0.1 M < IS < 1 M), hydrophobic interactions and ion bridging stabilized 3D-projected coils. The 3D conformation manifested through the increased number of superposed segments in Figure 1c,e,f. For the high concentrations (IS > 1M) of DC, the P2VP coils retained the 3D-projected state. Thus, multivalent counterions stabilize 3D-coils at high salt concentrations. Multivalent anions, which are strongly correlated at the PE backbone, cross-link the PE (effect of bridging), thereby preventing the complete reexpansion of polymer chains. The results are in accord with simulations and theory,<sup>23</sup> except with regard to the strong reexpansion in the presence of MC. The latter can be explained by strong van der Waals interactions of the pyridine ring with mica. These interactions lead to a near full recovery of the 2D-equilibrated coil conformation in the adsorbed P2VP chains.

In summary, this work provides direct experimental verification (on the level of single molecules) for the behavior of hydrophobic polyelectrolyte chains adsorbed at the solid–liquid interface in the full range of possible salt concentrations: (a) in a dilute salt solution, PE chains possess an extended coil conformation visualized as adsorbed 2D-equilibrated coils; (b) in a moderate salt concentration range, the polymer coil shrinks and approaches the dimensions of a polymer coil under  $\theta$ -conditions and the chains are visualized as adsorbed 3D-projected coils; (c) at high salt concentrations, the polymer coils reexpand and the molecules are visualized as 2D-equilibrated extended coils; however, (d) reexpansion is limited in the presence of multivalent counterions, presumably due to the bridging of the polymer coils by the counterions.

**Acknowledgment.** This work was supported by the NSF Grant CBET-0756461.

**Supporting Information Available:** experiment details and analysis of standard deviations. This material is available free of charge via the Internet at <http://pubs.acs.org>.

## References

- (1) Holm, C.; Joanny, J. F.; Kremer, K.; Netz, R. R.; Reineker, P.; Seidel, C.; Vilgis, T. A.; Winkler, R. G. *Adv. Polym. Sci.* **2004**, *166*, 67–111.
- (2) Dobrynin, A. V.; Rubinstein, M. *Prog. Polym. Sci.* **2005**, *30*, 1049–1118.
- (3) Dobrynin, A. V. *Macromolecules* **2005**, *38*, 9304–9314.

- (4) Beer, M.; Schmidt, M.; Muthukumar, M. *Macromolecules* **1997**, *30*, 8375–8385.
- (5) (a) Bloomfield, V. A. *Biopolymers* **1997**, *44*, 269–282. (b) Liu, S.; Muthukumar, M. *J. Chem. Phys.* **2002**, *116*, 9975–9982.
- (6) (a) Klos, J.; Pakula, T. *J. Chem. Phys.* **2005**, *122*, 134908. (b) Solis, F. J.; de la Cruz, M. O. *Europhys. J.* **2001**, *4*, 143–152.
- (7) Muthukumar, M. *J. Chem. Phys.* **2004**, *120*, 9343–9350.
- (8) Schiessel, H.; Pincus, P. *Macromolecules* **1998**, *31*, 7953–7959.
- (9) Levin, Y. *Rep. Prog. Phys.* **2002**, *65*, 1577–1632.
- (10) Grosberg, A. Y.; Nguyen, T. T.; Shklovskii, B. I. *Rev. Mod. Phys.* **2002**, *74*, 329–345.
- (11) Dobrynin, A. V. *Curr. Opin. Colloid Interface Sci.* **2008**, *13*, 376–388.
- (12) Nguyen, T. T.; Rouzina, I.; Shklovskii, B. I. *J. Chem. Phys.* **2000**, *112*, 2562–2568.
- (13) Hsiao, P. Y. *J. Chem. Phys.* **2006**, *124*, Art. No. 044904.
- (14) Hsiao, P. Y.; Luijten, E. *Phys. Rev. Lett.* **2006**, *97*, Art. No. 148301.
- (15) de la Cruz, M. O.; Belloni, L.; Delsanti, M.; Dalbiez, J. P.; Spalla, O.; Drifford, M. *J. Chem. Phys.* **1995**, *103*, 5781–5791.
- (16) Jia, P.; Zhao, J. *J. Chem. Phys.* **2009**, *131*, Art. No. 231103.
- (17) (a) Kiriy, A.; Gorodyska, G.; Minko, S.; Tsitsilianis, C.; Jaeger, W.; Stamm, M. *J. Am. Chem. Soc.* **2003**, *125*, 11202–11203. (b) Minko, S.; Kiriy, A.; Gorodyska, G.; Stamm, M. *J. Am. Chem. Soc.* **2002**, *124* (34), 10192–10197.
- (18) Gorodyska, G.; Kiriy, A.; Minko, S.; Tsitsilianis, C.; Stamm, M. *Nano Lett.* **2003**, *3*, 365–368.
- (19) (a) Roiter, Y.; Minko, S. *J. Am. Chem. Soc.* **2005**, *127*, 15688–15689. (b) Roiter, Y.; Minko, S. *J. Phys. Chem. B* **2007**, *111*, 8597–8604.
- (20) (a) Roiter, Y.; Jaeger, W.; Minko, S. *Polymer* **2006**, *47*, 2493–2498. (b) Minko, S.; Roiter, Y. *Curr. Opin. Colloid Interface Sci.* **2005**, *10*, 9–15.
- (21) Trotsenko, O.; Roiter, Y.; Minko, S. *J. Polym. Sci., Part B: Polym. Phys.* **2010**, *48*, 1623–1627.
- (22) Rivetti, C.; Guthold, M.; Bustamante, C. *J. Mol. Biol.* **1996**, *264*, 919–932.
- (23) Kundagrami, A.; Muthukumar, M. *J. Chem. Phys.* **2008**, *128*, Art. No. 244901.

JA106065G